A survey of fast power reduction methods for VSC connected wind power plants consisting of different turbine types

Arjen A. van der Meer, Ralph L. Hendriks, Wil L. Kling
Delft University of Technology
Mekelweg 4 2628 CD
Delft, the Netherlands
Tel.: +31 / (0) – 15 2788007
Fax: +31 / (0) – 15 2781182
E-Mail: A.A.vanderMeer@tudelft.nl
URL: http://www.ewi.tudelft.nl

Acknowledgements

This research was partly funded under the framework of the Dutch Ministry of Economic Affairs BSIK program 'Large-scale wind power generation offshore, towards an innovative and sustainable business,' with support from the We@Sea consortium (http://www.we-at-sea.org/).

Keywords

«Fault ride-through», «VSC-HVDC», «Fast power reduction», «Wind power plants»

Abstract

In this paper, a survey of fast active power reduction methods is given for improving fault-ride-through capabilities for wind parks that are connected to the grid through a voltage sourced converter (VSC) HVDC transmission scheme. In case of faults in the main grid, the limited current rating of the converter causes the direct voltage to rise quickly and hence fast reduction of generated power is required to keep the scheme in operation. This contribution studies the working principles of the power reduction methods on different turbine types and four particular cases with mixed turbine types have been studied. It turned out that frequency increase and voltage reduction is the most promising and cost-effective option. Furthermore it is shown that a combination of the proposed reduction methods leads to robust fault ride-through operation of the VSC-HVDC connected wind park.

Introduction

Voltage sourced converter (VSC) HVDC is a competitive concept for remotely located offshore wind parks [1]. This technology has several technical benefits when compared to line commutated converter (LCC) HVDC. Active and reactive power can be controlled independently, which makes 4 quadrant operation of the system possible. The use of power electronic switches with turn-off capability, such as the insulated gate bipolar transistor (IGBT), make it impossible for commutation failures to occur. The converter offers black start capabilities, which is crucial for operation of a wind park network. Moreover, there is a reduced requirement for harmonic filters, thus VSC stations can be built more compact than their LCC counterparts. This is especially beneficial for installation on offshore platforms. Negatively, the switching losses of VSC-HVDC are higher in comparison with LCC-HVDC and VSC-HVDC reliability has yet to be proven.

Riding through onshore grid faults poses a major challenge to the design of the VSC-HVDC connection [2]. During a severe voltage dip in the network, the power that the grid-side VSC (GSVSC) can deliver will suddenly decrease. Since the power generated by the wind turbine generators (WTG) is still being rectified by the wind park side VSC (WSVSC), the direct voltage will quickly rise to an unacceptably high level. Therefore, active power generated by the wind power plant must be decreased within a very short time interval, approximately 20 ms, depending on wind park size and DC-link capacitance.

Fault-ride-through methods for wind farms connected to the grid through VSC-HVDC have already been investigated [3, 4, 5, 6, 7]. In reference [3] several power reduction methods are compared. It was concluded that a combination of ride-through methods should always be used in order to survive a severe voltage dip at the grid side. It was not mentioned what kind of wind turbine generators had been used during the study, however. In [4], fault-ride-through capabilities of a VSC-connected wind park consisting of squirrel-cage induction generators (SCIG) was investigated and it was shown that a combination of voltage reduction and frequency increase led to adequate fast reduction of the active power injected into the DC circuit. In [5] and [6], power reduction is achieved by the application of fast communications between WSVSC and wind turbine. Ride-through of a wind park containing only doubly-fed induction generator based WTGs using frequency increase was studied in [7]

This paper combines the proposed power reduction methods for three commonly used types of WTG: Doubly-fed induction generator (DFIG), full converter generator (FCG) and squirrel cage induction generator (SCIG). Although wind park AC networks usually consist of one type of WTG, several configurations have been simulated to compare their dynamic behaviour.

The paper is organised as follows: First, the simulated network, WTGs and their associated controls will be described. Second, the power reduction methods will be briefly explained. Third, the power reduction methods will be applied to various topologies. The paper ends with conclusions and recommendations.

Network description

The network used for the fault-ride-through study is given in Fig. 1. The network consists of a 150 kV AC network node that is represented by an infinitely strong voltage source behind an impedance Z_g. It is connected to the GSVSC by transformer T1, whose leakage reactance has been combined with the grid impedance. The VSC-HVDC link consists of a 100 km long ±200 kV bipolar cable circuit. Cables have been modelled using their π-equivalent. A braking resistor (BR) can be included in the DC circuit for improved fault ride-through, as will be explained later. Each VSC adds a lumped DC capacitance to allow for operation as a STATCOM in case the cable is not available.

Dependent on the wind park rating, the wind park side AC collection network consists of 1 or more step down transformers. In this case, two transformers rated 300 MVA each. The wind park is assumed to connect at 150 kV voltage level to the offshore VSC station. The individual WTGs are connected to a 33 kV cable network. This voltage is stepped up to 150 kV at a centralised platform. Three different wind park sections have been modelled as aggregated WTGs of different type. All aggregated units are assumed to have equal rated power. The connection voltage of the WTGs is 690 V. A particular type of wind turbine can be excluded from the simulation by opening S1 to S3. Submarine cables have not been included in the model for sake of simplicity.

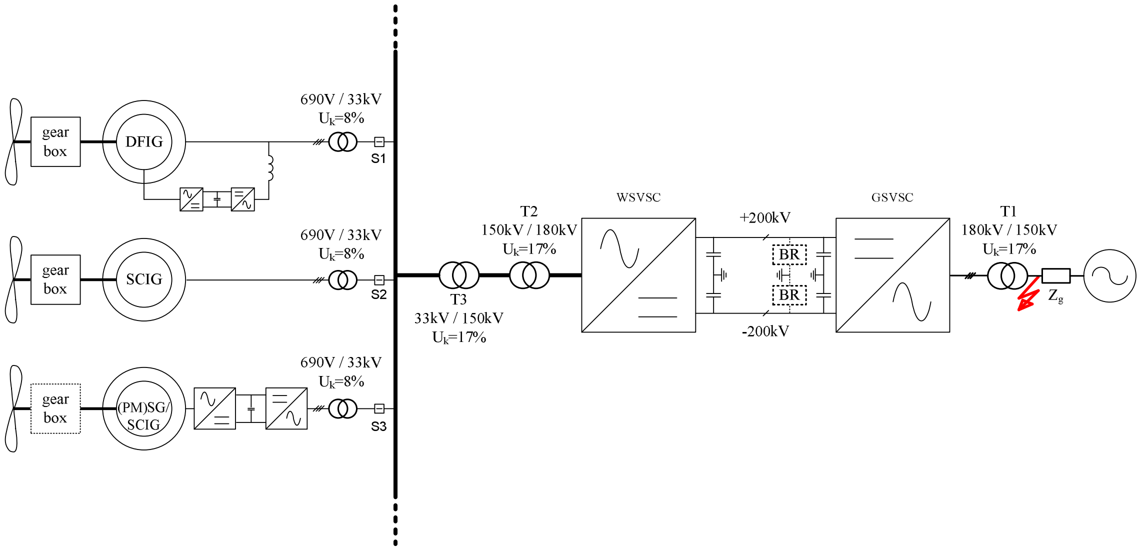

Fig. 1: Electrical system for a 300 MW VSC-HVDC connected wind park

VSC-HVDC

VSC-HVDC consist of power electronic switches with turn-off capability that are modulated by an appropriate pulse width modulation (PWM) scheme. The switching frequency in practical converters is in the range of 1–2 kHz. Usually, the switching effects are of a lesser importance for grid interaction studies as they are either filtered or are too small to have a significant influence on overall system behaviour, e.g. due to the application of multilevel converters [8]. Moreover, simulation of each particular switching element requires a very small time step size compared to those commonly applied in power system simulation software. Therefore, a fundamental-frequency model has been applied in this study, as has been proposed in [9, 10, 11]. In this study, the VSC-HVDC connection was modelled according to the averaged model, which represents the AC-side of WSVSC and GSVSC by a variable three-phase voltage source and the DC-side by a variable current source. The AC and DC side are linked by the active power balance equation.

A VSC-HVDC connection can be operated and controlled in different ways. First, if a VSC-HVDC connection for power exchange between two active AC-networks is involved, active and reactive power can be controlled independently by vector control [12]. One VSC-station controls the direct voltage while the other controls the active power flow; reactive power is controlled by both VSC stations in the same way. Second, if one of the AC networks is not an active network, as is the case for a wind park, one VSC station must be operated as a ‘slack node’ that provides a fixed voltage and frequency reference. The other VSC station then has the responsibility to balance the direct voltage [7].

DFIG

The majority of recently installed offshore WTGs are of the DFIG type [13]. As shown in Fig. 2, DFIG wind turbines contain a rotor connected back-to-back converter with a power rating of typically 30% of the WTG rating to enable (partial) variable speed operation.

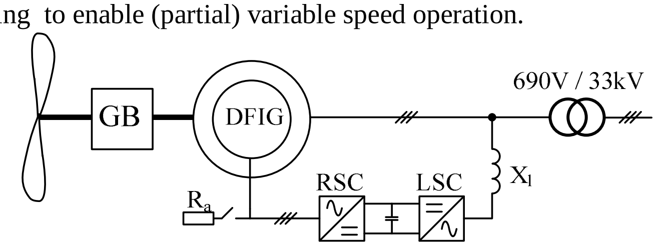

Fig. 2: Single line representation of DFIG wind turbine type

The dynamic model of the DFIG wind turbine was adapted from [14] and extended with converter control loops presented in [15]. The line side converter (LSC) controller inputs are obtained by three-phase network voltage and current measurements that have been transformed to the synchronously rotating reference frame. The rotor side converter (RSC) controller inputs are obtained by transformation of rotor voltages and currents to a reference frame that is rotating at slip frequency. During normal operation the LSC controls the direct voltage and operates at unity power factor while the RSC controls the active and reactive power exchanged with the offshore grid. Active power control is established by maximum power tracking (MPT) that controls the electrical torque to a predefined set point by regulating the rotor current [16]. For successful fault ride-through of the DFIG during voltage sags in the AC network, the rotor circuit is equipped with a crow bar protection mechanism. During network voltage sags high rotor currents (up to 4 per unit) might occur and could damage the converter. The crow bar connects an additional resistance R_a to the rotor and at the same time the RSC blocks.

SCIG

The first WTGs put in operation were fixed-speed machines consisting of SCIG directly connected to the grid. These WTGs operate at a (nearly) fixed rotational speed and therefore, energy extraction from the wind is optimised for only one particular wind speed. SCIG WTGs have the advantage to be very reliable and robust due to their simple construction and can therefore be regarded as a competitive alternative to variable-speed machines with power electronics, mainly for application offshore. However, a SCIG based wind turbine consumes reactive power over the complete operating range and that must be compensated in the wind park network. Moreover, active power can only be controlled by the relatively slow blade pitching mechanism which makes the SCIG wind turbine prone to grid disturbances.

The dynamic model of the SCIG is based on the equations found in [17]. Fixed-speed wind turbines can be equipped with active stall control or pitch control. Active stall control has the advantage that power can be reduced more quickly during grid disturbances, whereas pitch control is more robust due to its reduced sensitivity to mechanical disturbances [13].

FCG

FCG based wind turbines can apply different generator (synchronous, asynchronous), excitation system (electrical, permanent magnet), and gear box (two stage, single stage, direct drive) technologies. A power electronic converter interfaces the generator with the grid to allow operation over a wide speed range. An extensive comparison of recently developed and installed FCG WTGs is presented in [18]. The power electronic converter separates the generator and the rotating mass from the rest of the AC network. Electrical or mechanical transients that occur at the generator side are not reflected to the grid side and therefore a simplified model, which represents the generator by a variable torque source [19], might be applied.

The model is schematically presented in Fig. 3. The only differential equation describing the machine model is the equation of motion

$$\frac{d\omega_m}{dt} = \frac{T_m - T_e}{J} \tag{1}$$

where ω_m is the rotor speed, T_m is the shaft torque, T_e is the electromagnetic torque, and J is the moment of inertia of the lumped rotating mass.

The aim of the machine side converter (MSC) is to collect the power delivered by the generator, which is in practice achieved by controlling the generator frequency. The line side converter (LSC) controls the direct voltage and the reactive power delivered to the grid. As the electrical generator dynamics are omitted the current injected in the DC-link can simply be described as

$$I_{dc,WSC} = \frac{T_e \omega_m}{V_{dc}} \tag{2}$$

Here $I_{dc,WSC}$ represents the injected direct current. The LSC has been modelled according to the averaged model as described for the VSC.

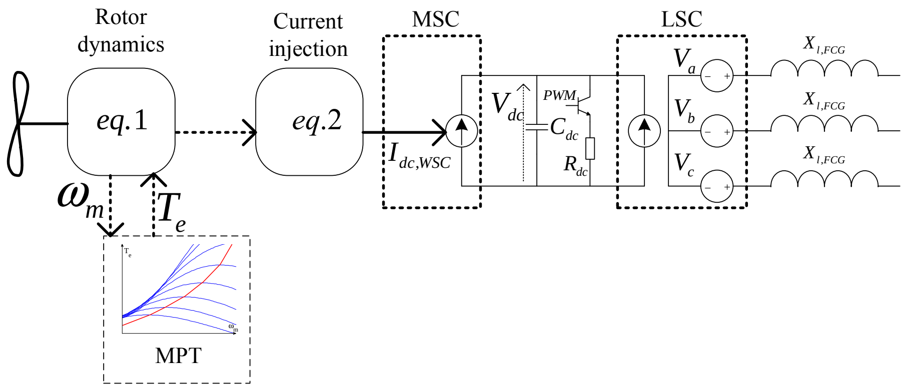

Fig. 3: Simplified model of a full converter generator.

During grid disturbances the LSC will run into its current limit and limited power exchange capacity with the AC network is available. In the presented model this is done by limiting T_e ,which results in a limited current injection and rotor acceleration. After voltage recovery, a high amount of energy will be injected into the DC-circuit; a DC-chopper with braking resistor R_{dc} was included in the model for dissipating this excess energy. In practice, a braking resistor is implemented also for the reason of high current flowing through the freewheeling diodes during network disturbances (this effect is not visible when applying the averaged converter model).

Aerodynamic en mechanical model

In this study, for all WTG types, the complete drive train is modelled as a lumped rotating mass. A lossless gearbox was assumed which is connected to the rotor blades by an infinitely stiff shaft. For simplicity, all WTG types are simulated using the same aerodynamic and mechanical model. The rotor aerodynamic model was developed based on the analytical expression for the C_p–λ– β curves given in [20].

During this study, the pitch controller depicted in Fig. 4 was used to reduce mechanical torque during grid disturbances or situations with wind speeds above nominal. The per unit rotor speed ω_m is compared to the maximum allowable rotor speed $\omega_{m,max}$. The introduced error signal e is amplified by a proportional amplifier with gain $K_{p,pitch}$. An integral controller was not included as the pitch controller is only operating during relatively short grid disturbances in which the control error e can hardly be regulated to zero. As can be seen, only positive pitch angles can be set as active stall control was not considered. The maximum pitch angle rate of change was set to 13°/s as this is commonly used for emergency braking and other situations that require a quick mechanical power reduction.

For fixed-speed wind turbines, $\omega_{m,max}$ must be set to a relatively small value compared to the value for variable speed wind turbines because SCIG are operating at a much smaller slip. To achieve equally high mechanical torque reduction for all wind turbine types, $K_{p,pitch}$ must have a higher value for fixed speed wind turbines.

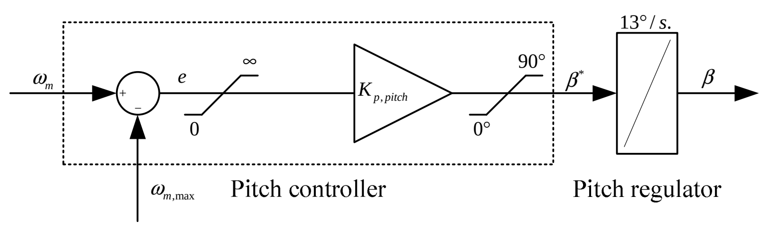

Fig. 4: Generic pitch angle controller and regulator used for each wind turbine type.

Power reduction methods

Depending on the HVDC link capacitance, only a few milliseconds are available for active power reduction at WSVSC. It must be noted that, though costly, extra capacitors can be installed to increase the time available to achieve correct fault ride-through of the wind park. Some power reduction methods require extra control loops within the WTGs. Reduced power exchange with the onshore network can be detected by the WSVSC by either a signal from the GSVSC through a communication link or by an elevated direct voltage at the wind park side of the DC-link. Combinations of fast power reduction methods are summarised in reference [3] and implemented in the models during this study. This paper focuses on power reduction methods on a conceptual level, hence detailed technical requirements of specific grid codes are not taken into account.

Wind park frequency increase

Frequency increase is a promising solution since power can be quickly reduced for each wind turbine type. SCIGs have a natural frequency response as the generator slip quickly decreases by raising the frequency by only a few percent, causing the active power output to drop near zero. DFIG and FCG based wind turbines do not respond naturally to a frequency deviation as their controls are designed to inject a fixed power into the network independent of the network frequency. To this end, a phase-locked loop (PLL) is applied that aligns the internal reference frame of the controller to the network voltage in a short time interval. Therefore, an additional control loop must be implemented into the existing converter controls that adds a droop characteristic as presented in [21]. It must be noted that the frequency measured by DFIG and FCG wind turbines is determined by PLL dynamics and so does the output power of the wind turbine.

Fig. 5 shows the DFIG and the FCG droop-regulator implementation. During frequency increase, the reference torque T_e acquired by MPT is decreased by a factor P^*, which results in the torque reference T_e^*. The per unit droop K is depending on the actual wind park configuration and should be high for the case of DFIG or FCG based WTGs that are installed in a wind park together with SCIGs.

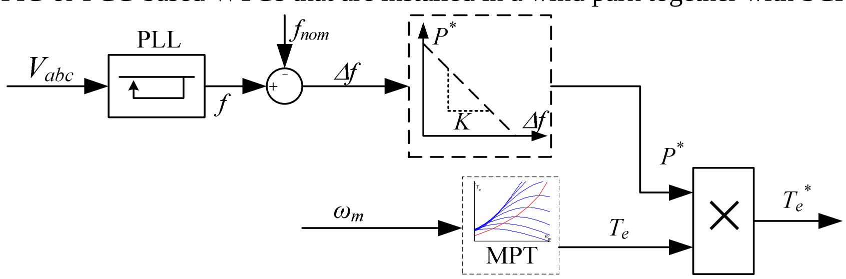

Fig. 5: Frequency control support of FCG and DFIG wind turbines during increased AC frequency

On the WSVSC side, the frequency increase is realised by adding an additional phase angle θ_a to the generated AC voltage vector. This is triggered by an abnormal direct voltage. As can be seen in Fig. 6 frequency increase is obtained here by controlling an additional phase angle θ_a according to

$$\theta_a = K_{p,f}\left(V_{dc} - V_{dc}^*\right) + K_{i,f}\int\left(V_{dc} - V_{dc}^*\right)dt \qquad (3)$$

with $K_{p,f}$ and $K_{i,f}$ the proportional and integral phase angle controller gain respectively, V_{dc} the HVDC link direct voltage, and V_{dc}^* the direct voltage set point which is equal to the nominal direct voltage in this case. The additional phase angle θ_a is added to the nominal frequency phase angle $2\pi ft$ to obtain the reference phase angle, and thus frequency for the converter modulator. Controller gains strongly depend on wind park configuration as highly FCG and DFIG penetrated wind parks have a well defined frequency response (by droop constant K), whereas the frequency response of SCIGs is dependent on slip and thus on operating point. After direct voltage recovery, the phase angle controller is disabled immediately and WSVSC switches back to normal operation.

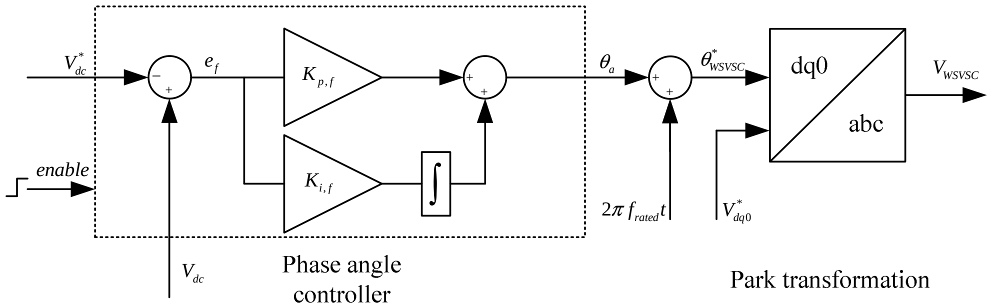

Fig. 6: Phase angle controller for frequency modulation during protection operation.

Offshore voltage reduction

Reduction of the wind park voltage will lead to a reduced wind turbine power production by natural response. FCG (and to a limited extent DFIG) WTGs will hit their current limit at low network voltages. Consequently, less active power will be fed into the offshore AC-network. In [4], voltage reduction was successfully applied for SCIG based wind parks. As the developed electromagnetic torque is proportional to the square of the AC voltage magnitude, active power will be reduced quickly. Due to the sudden change in electromagnetical torque the mechanical system will react heavily to abrupt voltage changes. For DFIG based WTGs triggering of the crow bar protection should be avoided in this case. Reference [6] proposes a new voltage reduction method based on direct magnetisation of DFIGs to avoid a high DC-component in the DFIG current that normally triggers the crow bar. In this study that method has not been applied however, and voltage reduction has been realised by a steep decrease of the WSVSC voltage reference. After direct voltage recovery, the reference signal is gradually restored to its pre-fault value.

Fast communication

Output power of wind parks consisting of FCG and DFIG can also be reduced by a fast communication link between the WSVSC and the individual WTGs [5], [6]. Referring to Fig. 6, P^* will be set to a limited value after detection of direct voltage elevation and will which consequently lead to a sudden decrease of active power production. The method is not well suited for wind parks consisting of SCIG since output power can only be reduced by pitching the blades, which is too slow. Disadvantages of communication links are the lower reliability and the inherent communication delay, which may be in the range of 10–100 ms. Therefore, the application of this method is not recommended [7] and should be utilised only in combination with one of the other fast power reduction methods.

DC braking resistor

Application of a braking resistor in the DC circuit has two particular advantages. Firstly, no further power reduction method has to be applied as excess DC-link energy is dissipated in the resistors that are rated for full power. Secondly, the offshore wind park can remain in full operation during any onshore grid disturbance and the WTGs experience no mechanical stresses during chopper operation. Reference [3] distinguishes between small braking resistors that are used in combination with other fast power reduction methods and large braking resistors, which are operating at full wind park power rating. The costs of implementing a braking resistor are mainly determined by the power electronics, which must capable of carrying the full current rating of the link in either case.

In this study, a braking resistor operating at nominal wind park power was applied for power reduction. After the protection circuit is triggered, the DC-chopper controls the direct voltage to a set point slightly above its nominal value as the GSVSC is switched into current limit mode.

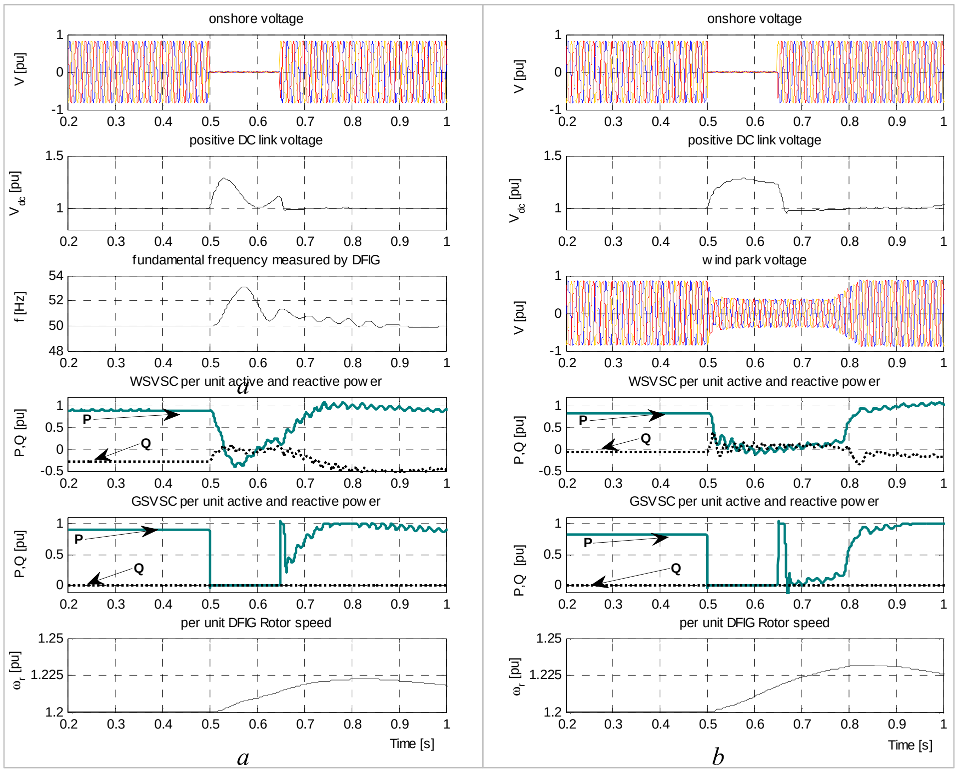

Fig. 7: (a) Fault ride-through of a wind park consisting of DFIG and SCIG based WTGs using frequency increase. (b) Fault ride-through of a wind park consisting of DFIG and FCG base wind turbines by fast communication and voltage reduction.

Simulation Studies

Simulations of the 300 MW VSC-HVDC connected wind park have been performed using Matlab/Simulink using the SimPowerSystems blockset. WTGs of the same type have been aggregated into single units in order to decrease model complexity. Moreover, a constant wind speed was assumed. Four cases have been studied:

- DFIG and SCIG based wind park with power reduction by frequency increase;
- DFIG and FCG based wind park with power reduction by fast communication and voltage amplitude reduction;
- FCG and SCIG based wind park with power reduction by communication, frequency increase, and voltage reduction;
- FCG and SCIG based wind park with power reduction through application of a braking resistor.

All four cases show the wind park response to a 150 ms bolted fault directly at the GSVSC terminals, initiated at *t*=0.5 s. This is considered the worst case scenario for ride-trough of the wind park. All power reduction methods are set to be triggered when the direct voltage exceeds its rated value by 3%.

In Fig. 7(a), FRT of a wind park consisting of DFIG and SCIG type wind turbines is successfully achieved by reducing the active power using frequency increase only. The modulated frequency should not differ more than 5% from the rated frequency because SCIG WTGs have a very steep natural frequency response: K_{pf}=0.5 and K_{if}=100 were chosen for the phase angle controller. The DFIG WTGs' measured frequency quickly increases and consequently, the wind park active power is substantially decreased. As can be seen, the direct voltage will not exceed its nominal value by more than 30%, which is assumed acceptable for a short time interval.

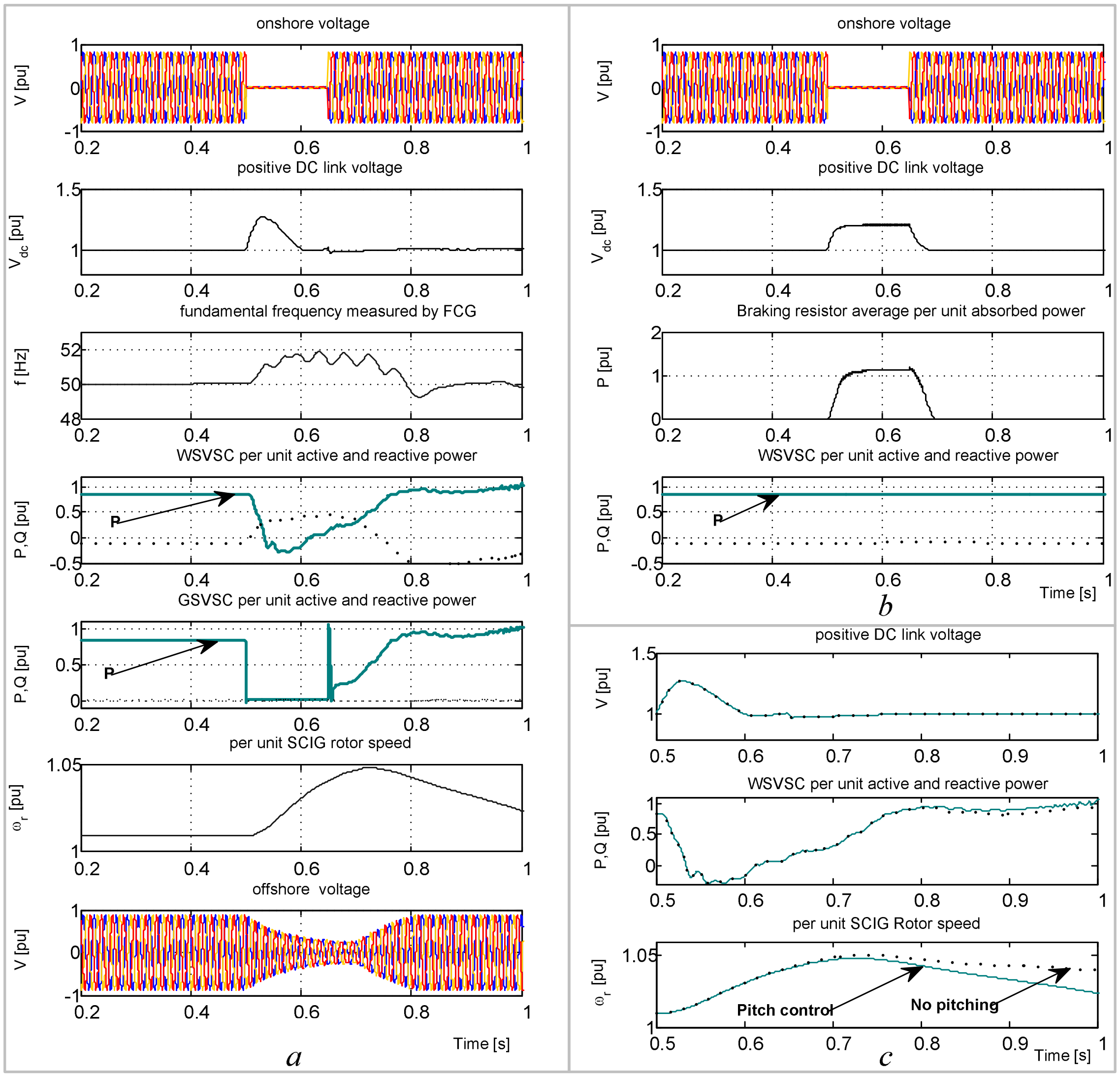

Fig. 8a: Fault ride-through of a SCIG and FCG based wind park using all methods except a braking resistor. b: Fault ride-through of the same wind park using a braking resistor only. c: The effect of the pitch regulator.

FRT of a DFIG and FCG based wind park by active power reduction trough fast communication and AC voltage reduction is shown in Fig. 7(b). A communication delay between WSVSC and WTGs of 20 ms was assumed. When the protection system is triggered, both power reduction methods are started simultaneously. The voltage amplitude is being reduced to 0.5 per unit. When the GSVSC switches back to normal operation after the fault, it suddenly delivers the full rated power to the onshore grid. In practice, the onshore power should be restored by ramping. Meanwhile, the WTGs power set points are restored to their prefault values and after 100 ms, the offshore voltage amplitude will gradually be restored to the rated wind park voltage level.

Fig. 8(a) shows the successful fault ride-through of a wind park consisting of FCG and SCIG WTGs using a combined operation of frequency increase, voltage decrease and communication links. After onshore voltage recovery, active power production is resumed by gradually increasing the wind park voltage and by regulating the frequency back to its nominal value.

Fig. 8(b) depicts a SCIG and FCG based wind park as well, but now a braking resistor in the DC-circuit was applied. After elevated direct voltage detection, the braking resistor was activated. As can be seen, excess energy is dissipated by the braking resistor and the direct voltage is kept constant below 1.2 per unit while the wind park continuously operates at the same power rating.

Finally, a comparison is made between a SCIG and FCG based wind park with and without pitch regulation. As can be seen in Fig. 8(c), pitch control does not contribute much to active power production during the short period of interest, i.e. the first 100 ms after detection of the onshore voltage sag.

Conclusion

This paper presented the application of four fast power reduction methods for VSC-HVDC connected wind parks consisting of different turbine types. No additional equipment needs to be installed for frequency increase and voltage reduction and therefore, these methods are considered as the most cost-effective fault ride-through solution. An additional frequency-droop characteristic must be implemented in the WTGs for frequency increase, which is an additional design constraint. Application of communication links is not recommended as a single solution because of communication delays and reliability issues. The most robust option is to include a chopper-controlled braking resistor in the DC link. The wind turbines will not suffer heavy mechanical stresses and the DC link is protected to all kinds of onshore and offshore faults. This solution is however very costly because the chopper must be rated for the full power of the link.

Four particular cases have been studied and fault ride-through during onshore voltage sag was successfully achieved. The investigated power reduction methods were implemented in simulation models and show that further optimisation can be achieved for more robust ride-through of wind parks. Furthermore, it can be concluded that pitch control has a negligible influence on fast active power reduction because of the relatively large time constants involved. A future refinement of the study would involve more detailed representation of the drive train.

References

[1] P. Bresesti, W. L. Kling, R. L. Hendriks, and R. Vailati, “HVDC connection of offshore wind farms to the transmission system,” *IEEE Transactions on Energy Conversion*, vol. 22, no. 1, pp. 37–43, 2007.

[2] L. Stendius and P. Sandeberg, “Large scale offshore wind power energy evacuation by HVDC light,” in *Proc. European Wind Energy Conference*, Brussels, Belgium, Apr. 2008.

[3] L. Harnefors, Y. Jiang-Hafner, M. Hyttinen, and T. Jonsson, “Ride-through methods for wind farms connected to the grid via a VSC-HVDC transmission,” in *Proc. Nordic Wind Power Conference*, Roskilde, Denmark, Nov. 1–2, 2007.

[4] A. Arulampalam, G. Ramtharan, N. Caliao, J. B. Ekanayake, and N. Jenkins, “Simulated onshore-fault ride through of offshore wind farms connected through VSC HVDC,” *Wind Engineering*, vol. 32, no. 2, pp. 103–114, 2008.

[5] L. Xu, B. R. Andersen, and P. Cartwright, “VSC transmission operating under unbalanced AC conditions – analysis and control design,” *IEEE Transactions on Power Delivery*, vol. 20, no. 1, pp. 427–434, 2005.

[6] C. Feltes, H. Wrede, F. Koch, and I. Erlich, “Fault ride-through of DFIG-based wind farms connected to the grid through VSC-based HVDC link,” in *Proc. 16th Power Systems Computation Conference*, Glasgow, Scotland, Jul. 14–18, 2008.

[7] L. Xu, L. Yao, and C. Sasse, “Grid integration of large DFIG-based wind farms using VSC transmission,” *IEEE Transactions on Power Systems*, vol. 22, no. 3, pp. 976–984, 2007.

[8] B. Singh, B. N. Singh, A. Chandra, K. Al-Haddad, A. Pandey, and D. P. Kothari, “A review of three-phase improved power quality AC–DC converters,” *IEEE Transactions on Industrial Electronics*, vol. 51, no. 3, pp. 641–660, Jun. 2004.

[9] V. Blasko and V. Kaura, “A new mathematical model and control of a three-phase AC-DC voltage source converter,” *IEEE Transactions on Power Electronics*, vol. 12, no. 1, pp. 116–123, 1997.

[10] J. Morren, S. W. H. De Haan, and J. A. Ferreira, “Model reduction and control of electronic interfaces of voltage dip proof DG units,” in *Proc. IEEE Power Engineering Society General Meeting*, vol. 2, Denver, CO, Jun. 6–10, 2004, pp. 2168–2173.

[11] R. L. Hendriks, G. C. Paap, R. Völzke, and W. L. Kling, “Model of a VSC-HVDC transmission scheme for wind farm connection for incorporation in power system stability studies,” in *Proc. 16th Power Systems Computation Conference*, Glasgow, Scotland, Jul. 14–18, 2008.

[12] L. Harnefors, “Control of VSC-HVDC transmission,” tutorial presented at the IEEE Power Electronics Specialists Conference, Rhodos, Greece, Jun. 15–19 2008.

[13] T. Ackermann, Ed., *Wind Power in Power Systems*. Chichester, UK: John Wiley & Sons, Ltd, 2005.

[14] J. Morren, “Grid support by power electronic converters of distributed generation units,” Ph.D. dissertation, Delft University of Technology, Netherlands, 2006.

[15] A. D. Hansen and G. Michalke, “Fault ride-through capability of DFIG wind turbines,” *Renewable Energy*, vol. 32, no. 9, pp. 1594–1610, 2007.

[16] R. Pena, J. C. Clare, and G. M. Asher, “Doubly fed induction generator using back-to-back PWM converters and its application to variable speed wind-energy generation,” *IEE Proceedings Electrical Power Applications*, vol. 143, no. 3, pp. 231–241, 1996.

[17] P. C. Krause, O. Wasynczuk, and S. D. Sudhoff, *Analysis of Electric Machinery and Drive Systems*. New York, NY: Wiley-Interscience, 2002.

[18] H. Polinder, F. F. A. Van Der Pijl, G.-J. De Vilder, and P. Tavner, “Comparison of direct-drive and geared generator concepts for wind turbines,” *IEEE Transactions on Energy Conversion*, vol. 21, no. 3, pp. 725–733, 2006.

[19] J. G. Slootweg, S. W. H. De Haan, H. Polinder, and W. L. Kling, “General model for representing variable speed wind turbines in power system dynamics simulations,” *IEEE Transactions on Power Systems*, vol. 18, no. 1, pp. 144–151, 2003.

[20] S. Heier, *Grid integration of wind energy conversion systems*. Chichester, UK: John Wiley & Sons, Ltd, 1998.

[21] J. Morren, S. W. H. de Haan, W. L. Kling, and J. A. Ferreira, “Wind turbines emulating inertia and supporting primary frequency control,” *IEEE Transactions on Power Systems*, vol. 21, no. 1, pp. 433–434, 2006.